

## Review

CO<sub>2</sub> electrocatalytic reduction to ethylene and its application outlook in food science

Yuxuan Ding,<sup>1</sup> Yixuan Dong,<sup>1</sup> Min Ma,<sup>1</sup> Lili Luo,<sup>1</sup> Xifan Wang,<sup>1</sup> Bing Fang,<sup>1</sup> Yixuan Li,<sup>1</sup> Libing Liu,<sup>1,\*</sup> and Fazheng Ren<sup>1,\*</sup>

## SUMMARY

The efficient conversion of CO<sub>2</sub> is considered to be an important step toward carbon emissions peak and carbon neutrality. Presently, great efforts have been devoted to the study of efficient nanocatalysts, electrolytic cell, and electrolytes to achieve high reactivity and selectivity in the electrochemical reduction of CO<sub>2</sub> to mono- and multi-carbon (C<sub>2+</sub>) compounds. However, there are very few reviews focusing on highly reactive and selective ethylene production and application in the field of electrochemical carbon dioxide reduction reaction (CO<sub>2</sub>RR). Ethylene is a class of multi-carbon compounds that are widely applied in industrial, ecological, and agricultural fields. This review focuses especially on the convertibility of CO<sub>2</sub> reduction to generate ethylene technology in practical applications and provides a detailed summary of the latest technologies for the efficient production of ethylene by CO<sub>2</sub>RR and suggests the potential application of CO<sub>2</sub>RR systems in food science to further expand the application market of CO<sub>2</sub>RR for ethylene production.

## INTRODUCTION

Fossil fuels have become the main source of energy to maintain the development of society since 1950, as well as the main source of atmospheric emissions of anthropogenic carbon dioxide (CO<sub>2</sub>). The year-round average atmospheric CO<sub>2</sub> concentration ranged from about 277 ppm (one per million) in 1750 to a projected 412 ppm in 2020, and the level of atmospheric CO<sub>2</sub> has been increasing every year, with a total global CO<sub>2</sub> emission of 32,284 million tons in 2020.<sup>1</sup> As a result of increasing global population growth, natural resource consumption, and geological disasters, the emission of greenhouse gases, mainly composed of carbon dioxide, has increased, which has caused global climate change and significant damage to the environment. If not controlled, it is highly likely to affect human survival and development. Therefore, advocating low-carbon living has become a daily action, which has attracted widespread attention to reduce CO<sub>2</sub> emission from the scientific community. Studies have shown that controlling CO<sub>2</sub> emission does not restrict social development. Between 2010 and 2018, several countries have remained economically growing while achieving significant reductions in emission.<sup>2,3</sup> Of all policies, controlling CO<sub>2</sub> emission and converting them into economically beneficial and reusable forms of carbon are effective solutions to the outstanding constraints in resource and environmental.

Driven by the rapid development of fuel cells and new energy vehicles, increasing research has focused on capturing and storing CO<sub>2</sub> for reduction to high-value-added mono- and multi-carbon (C<sub>2+</sub>) compounds, including formic acid (HCOOH), methane (CH<sub>4</sub>), ethylene (C<sub>2</sub>H<sub>4</sub>), and ethanol (CH<sub>3</sub>CH<sub>2</sub>OH), etc., through biocatalysis,<sup>4</sup> thermocatalysis,<sup>5</sup> electrocatalysis, photocatalysis,<sup>6–9</sup> etc. Electrochemical CO<sub>2</sub> reduction has received wide attention due to its mild reaction conditions, easy operation, and high reusability. Ethylene is an essential product of the petrochemical industry and is extensively applied in diverse fields, such as fruit and vegetable ripening,<sup>10</sup> pharmaceutical synthesis,<sup>11</sup> agricultural production,<sup>12</sup> and plant induction,<sup>13</sup> possessing tremendous economic and utility significance, which has become a popular topic for electrochemical CO<sub>2</sub> selective conversion product research in recent years. After more than a decade of electrochemical catalyst research on CO<sub>2</sub> reduction, metal catalysts have been classified into four categories according to the reduction products. The main reduction product of Au, Ag, Zn, Ga, and Pd is CO.<sup>14–16</sup> HCOOH<sup>17,18</sup> is mostly produced by Pb, Hg, In, Sn, and Bi, which are metal electrodes at high hydrogen evolution potential, whereas metal electrode with lower hydrogen evolution potential such as Ni, Fe, Pt, and Ti mainly produces H<sub>2</sub>.<sup>19–21</sup> Cu is considered to be the only metal electrode capable of producing hydrocarbons.<sup>22</sup> Meanwhile, for CO<sub>2</sub>RR to generate C<sub>2+</sub> products, CO<sub>2</sub> needs to undergo several chemosynthetic and physical processes, including CO<sub>2</sub> adsorption and activation, C–O bond breaking and C–C coupling, conformational rearrangement, and desorption.<sup>23</sup> And the whole CO<sub>2</sub> reduction process ( $x\text{CO}_2 + y\text{H}^+ + ye^- \rightarrow \text{C}_x\text{H}_y\text{-2nO}_{2x-n} + n\text{H}_2\text{O}$ ) requires sufficient energy to cross the energy barrier for the hydrogenation of intermediates such as \*CO. Although breakthroughs have been made in the basic research of CO<sub>2</sub>RR, it is remarkable that due to factors such as the inability to equivalently expand the laboratory technological achievements, the efficient CO<sub>2</sub>RR technology for generating ethylene in the laboratory cannot be effectively applied in practical life. Currently, it is urgent to promote the application of CO<sub>2</sub>RR technology.

<sup>1</sup>Department of Nutrition and Health, China Agricultural University, Beijing 100193, China

\*Correspondence: liulibing@cau.edu.cn (L.L.), renfazheng@263.net (F.R.)

<https://doi.org/10.1016/j.isci.2023.108434>



In this review, we hope to provide new ideas for the application of CO<sub>2</sub>RR technology. Ethylene is an important mediating factor in food science research, as applying a small amount of exogenous ethylene can regulate the ripening of fruits and vegetables, induce the enrichment of plant functional factors, etc. Therefore, we innovatively propose to extend the application of CO<sub>2</sub>RR from industrial production to food science. First, we summarize the recent research advances in the efficient electrocatalytic reduction of CO<sub>2</sub> to produce ethylene via nanoparticle surface-modified catalysts, then presenting the catalysts, electrolytes, and electrocatalytic reactors in order, with a focus on some representative nanostructures of copper-based catalysts, including catalyst modification methods, structure, and morphology, in addition to mechanism of action, followed by a prospective application of CO<sub>2</sub>RR in food science finally. The purpose of this article is to provide a review of the unique catalysts, electrolytic cells, and catalysts that have been used in recent years for the electrocatalytic CO<sub>2</sub>RR reaction to produce ethylene and to provide an outlook for the future application of CO<sub>2</sub>RR in food science, with a view to introducing promising "carbon neutralization" technology into agricultural development.

## SELECTIVE PRODUCTION OF ETHYLENE BY REDUCTION OF CO<sub>2</sub>

The selective reduction of CO<sub>2</sub> to C<sub>2</sub>H<sub>4</sub> process mainly relies on the carbon-carbon coupling of the key intermediates \*CO and \*CHO at adjacent metallic sites. However, the formation of C<sub>2</sub>H<sub>4</sub> is not easy for direct carbon-carbon coupling, which is limited by dipole-dipole mutual repulsions between adjacent intermediates.<sup>24</sup> Hence, the C-C coupling reaction is an indispensable step in the formation of C<sub>2+</sub> products and has become a breakthrough point to improve the selective reduction of CO<sub>2</sub> to ethylene. Scientists suppress competitive reactions from improving metal catalysts, electrolyte, and electrolytic cell to lower the energy barrier limit for C-C coupling and realize the enhancement of catalytic efficiency, as well as electrolytic cell stability.

### Cathode catalyst materials

In electrocatalytic CO<sub>2</sub> reduction, the class of metal catalyst relates to the type of the main final product. Cu is the only metal catalyst found to reduce CO<sub>2</sub> to the high-value-added C<sub>2+</sub> product, mainly because Cu inhibits the hydrogen evolution reaction (HER) and enhances the hydrogenation or C-C coupling of intermediates such as \*CO.<sup>25</sup> However, pure Cu has poor performance in electrochemical catalysis. Researchers improve the overall performance of Cu catalysts by modifying the Cu surface, designing steric structures, creating active sites and nanotechnological treatments, etc.,<sup>26,27</sup> to influence the adsorption performance of intermediates during the reaction to achieve higher selectivity for a single target product. This section will briefly describe and discuss some of the distinctive catalyst designs of last years.

The preliminary theoretical calculation study put forward the conclusion that "Cu(100) surface is more conducive to C<sub>2</sub>H<sub>4</sub> formation, while Cu(111) surface is more conducive to CH<sub>4</sub> formation," and has a profound impact on the catalyst design in subsequent studies. Whether it is the modification of catalyst morphology, surface properties, nanostructure, or the search for oxidation/reduction state equilibrium on the Cu surface, the aim is to enhance the reactivity area of the catalyst or improve the adsorption of intermediates, thus better enhancing the product selectivity and product yield performance of CO<sub>2</sub> reduction. Yang's group<sup>28</sup> innovatively proposed that electric field and thermal field have been utilized to promote catalytic reactions, as they can regulate the thermodynamic and kinetic barriers of reactions, and coat Cu nanoneedles with polytetrafluoroethylene (PTFE). As the PTFE coverage range or the applied bias voltage increased, the induced electric and thermal fields at the tip showed significant enhancement (Figure 1), thereby promoting \*CO adsorption and \*CO dimerization, ultimately achieving FE<sub>C<sub>2</sub></sub> >86% under some current densities exceeding 250 mA cm<sup>-2</sup>. The outstanding innovation of this work is to enhance the synergistic electric-field-facilitated C-C coupling through the conformal coating of PTFE of Cu nanoneedles, thereby achieving the selectivity and reactivity of Cu-based catalysts for C<sub>2</sub> products, which is worth trying on the same type of catalysts. Wakerley's research team is inspired by the hierarchical structure of gas-trapping cuticles on subaqueous spiders, using monolayers of waxy alkanethiols to modify dendritic Cu nanoparticles to enhance their surface hydrophobicity, resulting in a significant increase in the Faraday efficiency (FE) of mono- and multi-carbon products. However, the rate of multi-carbon production decreased continuously due to the impact of air dendrite surface of the electrode.<sup>29</sup>

Choi's group designed Cu nano-catalysts with Cu(511) planar [3(100)×(110)] gradient surfaces (A-CuNWs). Because A-CuNWs can maintain a high-index A-(hkl) surface structure for a long time, it is not only more advantageous than Cu(100) or Cu(111) in thermodynamics but also has a higher barrier to the C1 pathway, which is not conducive to HER.<sup>30</sup> Compared with Cu(100), the step sites on Cu(511) can secure a higher local CO surface population and OH<sup>-</sup> adsorption, so it can stably produce ethylene (61%–72% FE<sub>ethylene</sub>) within 205 h. Importantly, the high-index A-(hkl) Cu surface is more advantageous than the Cu(100) surface in ethylene production, which is inconsistent with the theory that "Cu(100) surface is more conducive to ethylene formation" proposed in the previous theoretical calculation study. Zhang's group created nano-defective (2–14 nm) Cu nanosheets as catalysts in an electrochemical reduction method<sup>31</sup> (Figure 2G). This catalyst maintains the same species of Cu<sup>0</sup> throughout the whole electrocatalytic process. And the presence of a large number of atomic defects produces a concentration effect that favors the adsorption, enrichment, and restriction of key reaction intermediates (\*CO and \*OCCO) and OH<sup>-</sup>. The defective Cu(111) surface also lowers the energy barrier, ultimately facilitating the CO dimerization process and the production of ethylene. Most importantly, the nano-defective Cu(111) surface in this study can also achieve better ethylene selectivity, which is inconsistent with the theory that "Cu(111) surface is good for CH<sub>4</sub> generation" proposed in the previous theoretical calculation study. Based on the comprehensive research of Choi and Zhang, the conclusions of the previous theoretical calculations can be refuted. The subsequent research<sup>33</sup> also proves that the high-index surface is more advantageous to the generation of multi-carbon products and has more economic value. The future catalyst design ideas can be changed to seek the high-index surface.

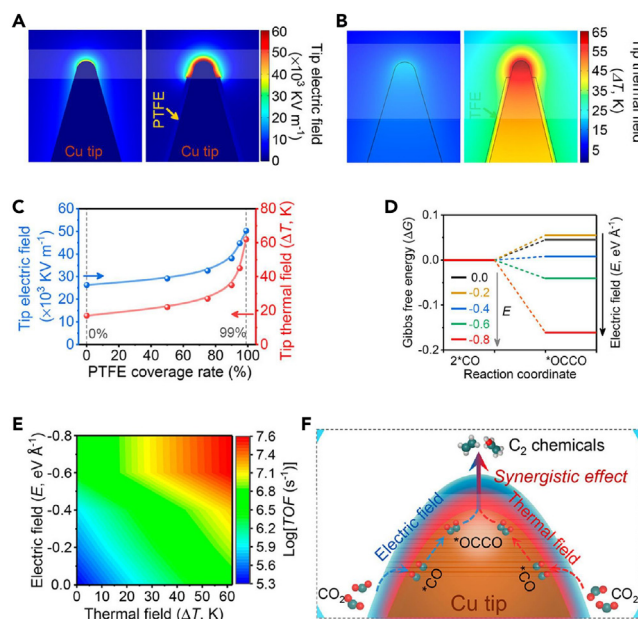


**Figure 1. FEM simulations and DFT calculations on a pristine Cu NN (tip) and a Cu NN with 99% PTFE coverage** (A–C) Distribution of electric and thermal fields on a pristine Cu NN (left) and a Cu NN with 99% PTFE coverage (right). (D–F) The mechanism of promoting C<sub>2</sub> formation by different electric and thermal fields.<sup>28</sup>

In contrast, Liu's research team prepared oxide-derived Cu (OD-Cu) catalysts with dense vertically layered Cu nanostructures (DVL-Cu), using constant current anodic oxidation and *in situ* electrochemical reduction.<sup>34</sup> DVL-Cu was able to exist and maintain Cu/Cu<sub>2</sub>O composite structures and subsurface Cu<sup>+</sup>, which can reduce the C-C dimerization energy in the ethylene formation pathway and suppress hydrogen evolution at higher overpotentials. Therefore, the catalyst was able to maintain stable electrolytic performance in KCl electrolytes for 55 h, and  $FE_{\text{ethylene}}$  is also maintained above 60%. Compared with the silicon Cu catalyst, DVL-Cu catalyzes CO<sub>2</sub> reduction to generate ethylene under milder electrolysis conditions, with higher  $FE_{\text{ethylene}}$ , and lower required current density. Because the Cu surface undergoes a dynamic reduction/re-oxidation behavior mechanism of Cu<sub>2</sub>O-CuO<sub>x</sub>-Cu which allows the catalytic reaction to be recyclable and potentially extends the useful life of the catalytic system by controlling the temperature as well as HCO<sub>3</sub><sup>-</sup> content.<sup>35</sup>

In addition, researchers have used innovative synthetic methods from lithium batteries and supercapacitors in the design of catalysts, which may lead to the discovery of new highly efficient Cu catalysts. Song's group introduced carbonized cellulose-modified carbon substrates and used carbon thermal shock (CTS) to create Cu nanocatalysts with high surface coverage (up to 85%) on a carbon substrate<sup>32</sup> (Figures 2A–2F), which increased the number of sp<sup>3</sup> defect sites in the Cu/cellulose/carbon paper catalysts. Due to the high surface coverage of Cu nanoparticles (NPs) and the high hydroxide (OH<sup>-</sup>) ion concentration provided by a highly alkaline electrolyte which promoted the C-C dimerization in the reaction, the system achieved a selectivity of approximately 49% for ethylene at  $-0.529$  V<sub>RHE</sub> and 10 M KOH electrolyte. Meanwhile, the cellulose/CP protection allowed the morphology of the Cu NPs to remain basically unchanged during the reaction, so that the stability of the system made more than 30 h. The polyelemental alloy NP materials introduced in this study have made breakthroughs in improving the stability of carbon-based electrodes, but the corrosiveness and recycling environmental protection of strong alkaline electrolytes for electrolytic cells still need to be explored.

Presently, there have been more researches on enhancing the catalytic performance by regulating the reaction morphology, interfacial oxidation state, and dopants of Cu, but few researches have been carried out on enhancing the catalyst performance through molecular modulation. Li's research team used organic molecules (include 12 N- arylpyridinium salts) to modify the electrocatalyst surface,<sup>36</sup> which resulted in higher ethylene selectivity, more stable intermediate \*CO, and lowest potential barrier for CO dimerization atop: bridge due to the electron donating capacity and nitrogen atoms of tetrahydro bipyridine. The  $FE_{\text{ethylene}}$  of Cu-12 (12 is N,N'-(1,4-phenylene) bipyridine salt) was 72% when the voltage was  $-0.83$  V. It is noteworthy that the membrane electrode assembly system could run continuously for 190 h at a full-cell voltage of 3.65 V with  $FE_{\text{ethylene}}$  maintained at 64%, which is much better than the best case  $FE_{\text{ethylene}} = 60\%$  reported in 2019. Meanwhile, some researchers have introduced polymers or organic functional groups into catalyst optimization to improve the variety and density of adsorbed species on the catalyst surface in order to enhance CO<sub>2</sub> reduction activity. Chen's group used pentafluoro phenyl acrylate as monomers to polymerize and methylate in order to obtain polymers with different degrees of species methylation. Different Cu-polyamine catalysts were prepared by co-plating. Due to the presence of amino groups, the modified electrode Cu-P1 increases the amount of activated CO on the electrode surface, local pH, and the stabilization of intermediates, thereby enhancing the catalyst's activity for CO<sub>2</sub> reduction. However, a more concentration alkaline electrolyte can reduce the overpotential at the anode, thus improving energy efficiency, resulting in

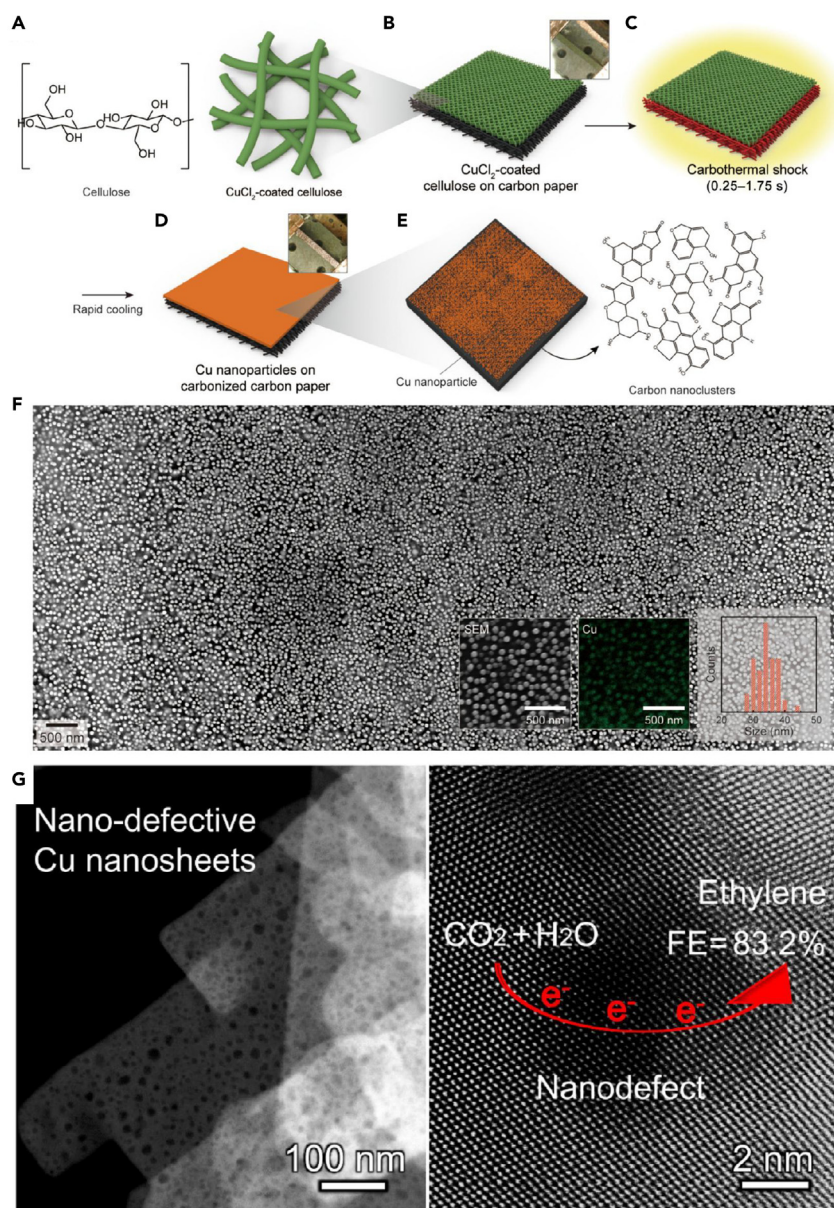


**Figure 2. Unique nanostructures of copper-based catalysts**

(A–F) Preparation process and low-magnification SEM images of the catalyst (Cu/Cellulose/CP).<sup>32</sup>

(G) HAADF-STEM images of n-CuNS.<sup>31</sup>

FE<sub>ethylene</sub> > 70%.<sup>37</sup> Lim's research team functionalized the surface of Cu by introducing a unique group (amine group) of histidine,<sup>38</sup> resulting in FE<sub>ethylene</sub> up to 76.6% and a device performance stability of 48 h at  $-2.0V_{RHE}$ . Furthermore, it is noteworthy that histidine has been specifically adsorbed to the Cu-Hist surface during CO<sub>2</sub>RR process and that the C-C coupling between histidine-bound \*CO and \*CHO is more favorable both mechanically and thermodynamically than that of \*CO-\*CO and \*CO-\*CHO (Figure 3). The formation of Hist-CO intermediates and the presence of C-N coupling provide an alternative route for CO<sub>2</sub> to generate C<sub>2+</sub> products, so the present catalyst is more selective for C<sub>2</sub>H<sub>4</sub> than CH<sub>4</sub>. The cationic effect on the catalyst surface,<sup>39</sup> together with the increased species and number of \*CO species, also provide favorable conditions for increased CO<sub>2</sub>RR generation of C<sub>2+</sub> products.

The use of organic molecules as passivators has been widely used in the development of high-efficiency perovskite solar cells, and excellent results have been achieved, but in recent years it has begun to be used in CO<sub>2</sub>RR. Although, passivation molecules can delay the corrosion rate of metal catalysts and improve their product selectivity. The binding of Ni to cyano(-CN) groups is an optimization method that has been widely studied and has achieved excellent stability (conversion frequency of 22,000 h) as well as selectivity (FE<sub>CO</sub> ≥ 90%).<sup>40</sup> But its service

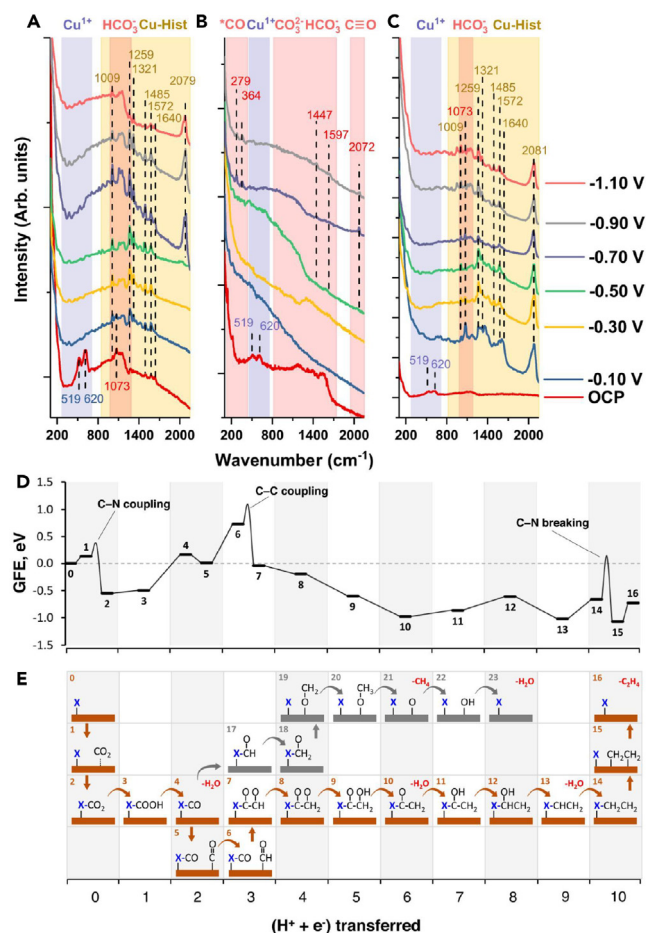


**Figure 3. Mechanism of organic functional group modified copper-based electrode to improve the selectivity of C<sub>2+</sub> product**  
(A–C) *In-situ* Raman spectroscopy on bare and histidine functionalized Cu<sub>2</sub>O under CO<sub>2</sub>RR relevant conditions.  
(D–E) Mechanistic understanding of favorable and unfavorable CO<sub>2</sub>RR pathways on Cu-Hist calculated by DFT.<sup>38</sup>

life and performance stability are still not outstanding due to the study of the passivation mechanism of electronic defects on the surface of grain boundaries, the complexity and diversity of materials, and the inability to effectively passivate the working electrode as a whole.

In recent years, for CO<sub>2</sub> reduction reactions, as CO is a key intermediate of CO<sub>2</sub>RR, CO<sub>2</sub> electrolytic cells are designed to reduce CO<sub>2</sub> to CO first and then to ethylene by CORR. The proposed CuO<sub>x</sub>-NiNC (1:2 or 1:4) tandem catalysts with CO<sub>2</sub>/CO gas by Wang's group proved significantly improved C<sub>2</sub>H<sub>4</sub> catalytic performance compared with the loaded CuO<sub>x</sub> NPs,<sup>41</sup> while still having the same C<sub>2</sub>H<sub>4</sub> yield even with reduced CuO<sub>x</sub> loading on the tandem catalyst. Due to the fact that co-fed CO does not compete with CO<sub>2</sub> for adsorption sites, local CO<sub>(g)</sub> concentration increases, resulting in enhanced \*CO coverage and dimerization rate. This further leads to more and more energy advantages in the cross-coupling CO<sub>2</sub>-CO reaction pathway, thereby enriching the pathway of C<sub>2+</sub> product generation. Moreover, the relative selectivity of the C<sub>2+</sub> products was largely independent of the overall coverage of CO on the Cu surface. And in the latest study, the main group single-atom catalyst (SACs) Ca-NO<sub>3</sub> can change the surrounding electron localization through asymmetric coordination, thereby promoting the formation of \*COOH and achieving FE<sub>CO</sub> ≥ 90%. The research is groundbreaking, going beyond the range of commonly used metal catalysts and achieving extremely high CO selectivity and device stability,<sup>42</sup> illustrating that perhaps the limitation of developing CO<sub>2</sub>RR catalysts only on Cu may be broken through, and tandem catalysts can become an important thrust for the development and improvement of catalytic performance of future CO<sub>2</sub>RR catalysts. In addition, these studies have been shown that CORR and CO<sub>2</sub>RR can mutually promote ethylene production to a certain extent,<sup>39,41</sup> whereas cobalt phthalocyanine is currently used in both CO<sub>2</sub>RR and chlorine-containing solution treatment. Ren's research team broke the once accepted view that "molecular catalysts cannot be electrolyzed at commercially relevant rates of product formation rates" and identified commercial cobalt phthalocyanine (CoPc) as a homogeneous electrocatalyst with high CO selectivity (>50%) at low current densities (<40 mA/cm<sup>2</sup>) in both flow cells<sup>43</sup> (Figure 4). The CoPc modification not only improves the selectivity of CO<sub>2</sub> for CO, but also for contaminated water containing 1,2-dichloroethane (DCA), multi-walled carbon nanotube (CNT) catalysts with CoPc molecules attached can achieve FE<sub>ethylene</sub> close to 100% and DCA removal >95% at a certain voltage.<sup>44</sup> Therefore, such studies may lead to a better choice of catalysts and electrolytes.

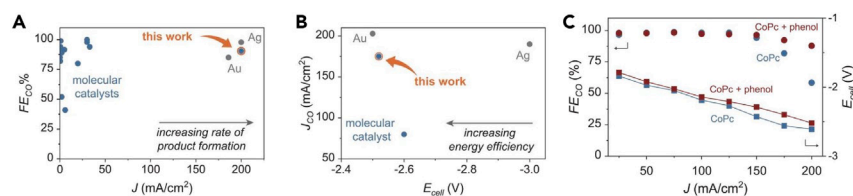


**Figure 4. CO<sub>2</sub>RR selectivity for CO formation as a function of current density and cell voltage**

(A and B) Selectivity and activity for CO production as a function of current density and cell voltage for molecular and heterogeneous CO<sub>2</sub>RR electrocatalysts. (C) CO<sub>2</sub>RR selectivity for CO formation and applied voltage as a function of current density.<sup>43</sup>

### Input gases and electrolytes

Through research on the reaction interface, Cu surface morphology, and CO<sub>2</sub> reactivity, it has been established that both CO<sub>2</sub>RR and CO reduction reaction (CORR) occur at the cross-section between the metal electrode and the aqueous electrolyte,<sup>45</sup> thus the catalytic performance is influenced by both the electrode surface and the electrolyte. However, current research has mainly focused on electrocatalyst development and electrolytic cell optimization, with few studies on the pathways of surface-mediated catalytic reactions<sup>39</sup> influenced by input gases<sup>41,45</sup> and electrolyte cations. The electrolyte provides a medium for the transfer of protons and electrons in the electrocatalytic reaction, while the input gas determines its reaction pathway. Hence, the impact of the selection of electrolyte and input gas on the CO<sub>2</sub>RR cannot be ignored.

In addition to the experiments conducted by feeding pure CO<sub>2</sub> gas, scientists have started new research on the gas feedstocks passed into the electrolytic cell in terms of conforming to the practical application environment, improving the CO<sub>2</sub>RR efficiency and multiple gas utilization. Since incomplete combustion of industrial fuels produces a mixed CO/CO<sub>2</sub> gas, Wang's group<sup>41</sup> designed a CuO<sub>x</sub>-NiNC (1:4 or 1:2) tandem catalyst for experiments using CO<sub>2</sub>/CO as the gas feedstock. Notably, after quantitative analysis of the C<sub>2</sub>H<sub>4</sub> formation pathway, they found that the CO<sub>2</sub>-CO pathway in the \*CO dimerization reaction has a relative charge contribution of 45% and that the kinetic activation potential of the catalytic CO-C<sub>2</sub>H<sub>4</sub> cascade is lower than that of CO<sub>2</sub>-C<sub>2</sub>H<sub>4</sub>, so that CO in the feedstock can increase ethylene production via the cross-coupling pathway, while inferring that the rate of ethylene production is more likely to be related to the kinetic mechanism rather than due to catalytic factors.

He's group<sup>45</sup> feed a mixture of CO<sub>2</sub> and O<sub>2</sub> in different molar ratios (9:1 or 8:2) and pure CO<sub>2</sub> separately into an H-type electrolytic cell to react with carbon fiber paper deposited with polycrystalline Cu powder as the working electrode. It was found that the rates of some C<sub>1</sub> and all C<sub>2+</sub> products in the CO<sub>2</sub>RR reaction were significantly increased due to the promoting effect of oxygen reduction reaction (ORR) on CO<sub>2</sub>RR, when a certain amount of O<sub>2</sub> was present in the gas, in which the production rate of ethylene was elevated 4- to 216-folds (Figures 5A–5F). However, it should be noted that when electrolyzed for a long time, intermediates and products of different reduction pathways of ORR may have adverse effects on the CO<sub>2</sub>RR, including the depletion of the Cu electrode and electrolytic cell by the ORR product H<sub>2</sub>O<sub>2</sub>. The co-electrolysis of CO<sub>2</sub> with oxidants will cause an increase in electrolyte pH in the later stages, thus promoting hydrogen precipitation reactions. Such problems may be overcome by using a flowing electrolytic cell or changing to the acidic electrolyte.

The aforementioned studies shed light on the potential of different feedstock ratios of reaction gases to improve ethylene selectivity of electrocatalytic CO<sub>2</sub>RR. It is well known that \*CO dimerization on Cu(100) facets is more favorable; therefore, most catalyst modifications choose to construct more Cu(100) facets. However, the Cu(100) facets are less stable than the Cu(111) facets and prefer to reconstituting to the Cu(111) facets during electrocatalysis, which is still a non-negligible issue.<sup>46</sup> Nevertheless, higher CO partial pressures can open another coupled \*COOH and \*CO pathway to C<sub>2</sub>H<sub>4</sub> on the non-Cu(100) facets, and with extensive coverage of \*CO and locally high CO<sub>(g)</sub> concentrations, the pathway becomes increasingly energetically favorable<sup>41,45</sup> (Figures 5G and 5H), which may provide an optimized new pathway for the reduction of CO<sub>2</sub> to ethylene.

In electrochemical CO<sub>2</sub>RR studies, cations in the electrolyte were found to stabilize the adsorption of reaction intermediates on the catalyst surface, while their cumulative generated local electric field was able to reduce the energy of C-C coupling to form C<sub>2+</sub> products.<sup>47</sup> Studies have proved that the anion (OH<sup>-</sup>) generated in the reaction can be neutralized by HCO<sub>3</sub><sup>-</sup> or HPO<sub>4</sub><sup>2-</sup>. H<sub>2</sub> is the main product in K<sub>2</sub>HPO<sub>4</sub> solutions, whereas hydrocarbons and alcohols are more likely to be produced in non-buffered solutions such as low concentrations of KHCO<sub>3</sub> and KCl, mainly because these two types of solutions are less able to neutralize the anion, which leads to an increase in local pH and inhibits the HER. Furthermore, the overpotential of C<sub>2+</sub> products under alkaline electrolytes is substantially reduced, which is more conducive to the selection of multi-carbon products for the electroreduction process,<sup>48</sup> but strong alkaline electrolytes are demanding and unstable for the electrolytic cell, so 0.1 M KHCO<sub>3</sub> is the most commonly used electrolyte. Electrochemical CO<sub>2</sub>RR over Cu<sub>2</sub>O/Cu catalysts under bubbling and high-pressure conditions correlates strongly with the CO<sub>2</sub> (aq) concentration in the KHCO<sub>3</sub> electrolyte and slows down CO<sub>2</sub> dissolution and accelerates up desolvation when the solution salt fraction increases or the solute content increases<sup>49</sup> (Figure 6). When the electrolyte is an alkaline solution such as KOH, it can reduce the activation potential of C-C coupling by activated CO on the surface of the Cu electrode, effectively improving the efficiency of CO<sub>2</sub> reduction to generate ethylene,<sup>37</sup> but the corrosive effect of the alkaline electrolyte can affect the reproducibility of the electrolytic cell, which may be improved by using PTFE-based electrodes instead of carbon-based electrodes.

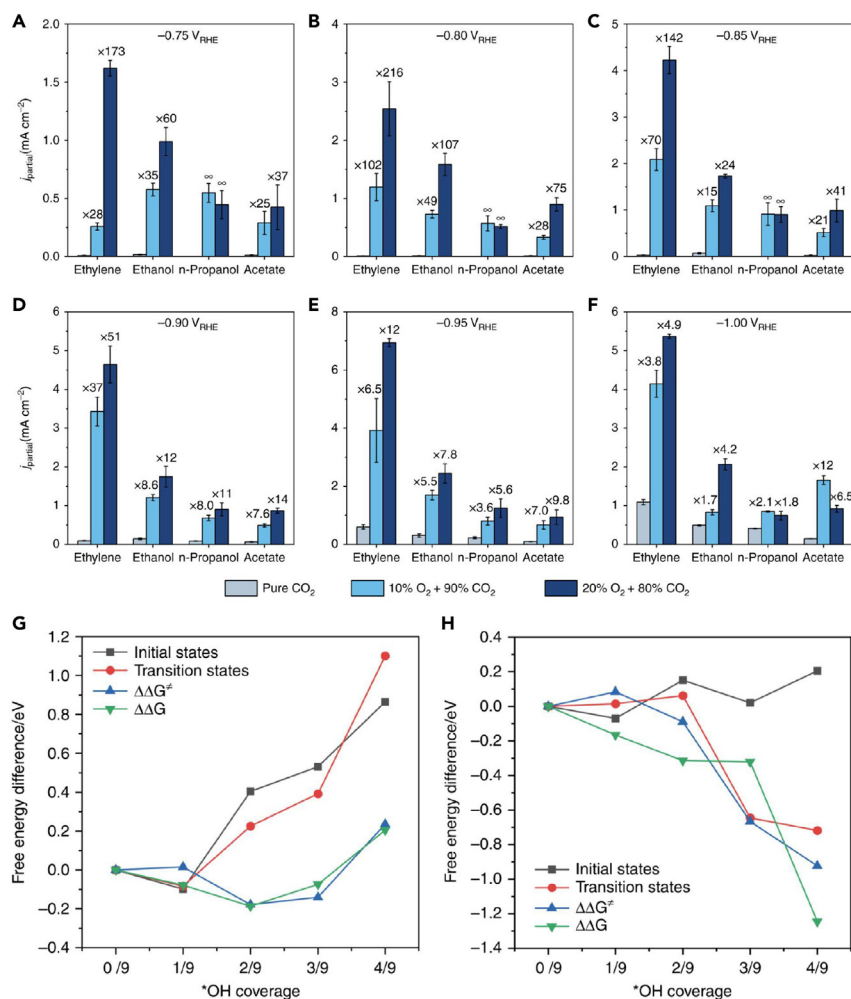


**Figure 5. Effect of CO<sub>2</sub>/O<sub>2</sub> reactant co-feed on CO<sub>2</sub>RR reaction**

(A–F) Effect of different molar ratios of CO<sub>2</sub> and O<sub>2</sub> gas on the formation of C<sub>2+</sub> products.

(G and H) Free energy diagram for CO<sub>2</sub>/O<sub>2</sub> reactant co-feeds. [(G) \*CO dimerization; (H) \*CO hydrogenation].<sup>45</sup>

With the application of different catalysts and electrolytic cells, researchers have selected new electrolytes for electrochemical CO<sub>2</sub>RR reactions based on the characteristics of the catalysts or electrolytic cells and achieved better reduction results. Among them, Zhang's research team<sup>31</sup> fabricated nano-defective Cu nanosheets (n-CuNS) by designing the atomic defects so that the stability of n-CuNS is examined at  $-1.18$  V (versus RHE) and  $0.1$  M K<sub>2</sub>SO<sub>4</sub> electrolyte conditions, and the FE<sub>ethylene</sub> was stable at 80% for 14 h. Moreover, the morphology of the nano-defective nanosheets was intact after 14 h. In contrast, Li's group<sup>50</sup> adopted an alkaline polymer electrolyte (QAPPT film) as the cathode gas diffusion electrode electrolyte and pure water as the anode electrolyte, with the Cu-QAPEEK-GDE three-phase interfacial structure providing a locally high current density and high electrochemical reaction interface, thus enabling an increase in FE<sub>ethylene</sub> at a reduced cell voltage and raised current density. This attempt of a cathode solid electrolyte breaks with the tradition of using liquid electrolytes and can tremendously simplify the device structure and increase its production efficiency.

As the diversification of the selection of electrolyte and input gas, the replacement of liquid electrolytes by polymer electrolytes will become a new highlight in electrochemical technology.

### Electrocatalytic reactors

Another effective way to improve the catalytic performance of CO<sub>2</sub>RR is the rational design and optimization of the electrolytic cell reactor. Early studies were typically conducted in hermetically sealed electrolytic cells. Due to the inability to separate the anode and cathode chambers, the reduction products will contact the anode and undergo oxidation again, so they are gradually replaced by H-type cells, where the two chambers could be separated by an ion exchange membrane and different electrolytes could be used. Subsequently, flow electrolytic

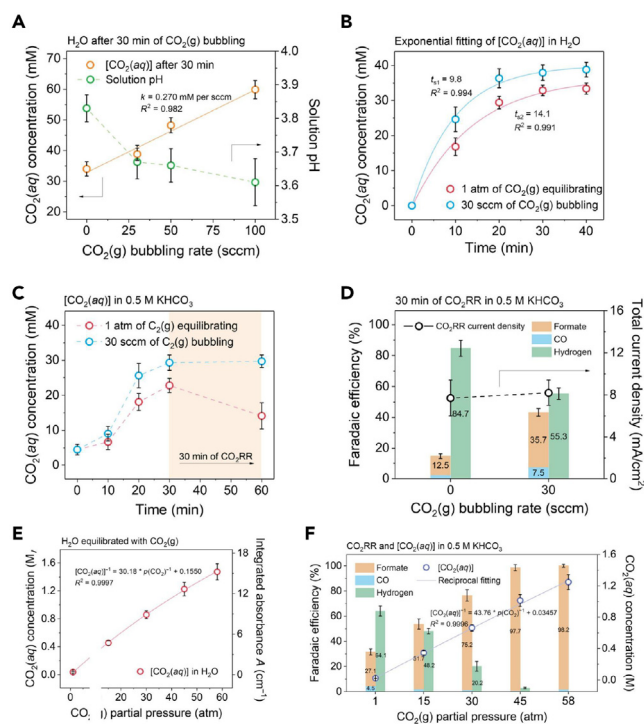


**Figure 6. The effect of  $\text{CO}_2$  (aq) concentration on  $\text{CO}_2\text{RR}$**   
(A–D) Dynamic changes of  $\text{CO}_2$  solvation in  $\text{H}_2\text{O}$  and 0.5 M  $\text{KHCO}_3$ .  
(E and F) The correlation between dynamic  $\text{CO}_2$  and high-pressure  $\text{CO}_2\text{RR}$ .<sup>49</sup>

cells offer superior catalytic and stability performance compared with H-type cells because of their high mass transfer efficiency,<sup>51</sup> whereas membrane electrode assembly (MEA)-based electrolytic cell systems also provide the same advantages as they do not use aqueous electrolytes. Furthermore, flow electrolytic cells and MEA-based electrolytic cell systems provide the possibility for reduction reactions at industrial current densities ( $>100 \text{ mA cm}^{-2}$ ). In this section, a brief overview of the different reactors will be given and discuss the advantages and disadvantages of the three reactors mentioned earlier based on example data, using the electrolytic cell stability performance and ethylene production efficiency as the main indicators.

### H-type electrolytic cells

Currently, most of the research still use H-type electrolytic cell as the main electrochemical device because of the advantages of low cost and operational difficulty. The ion exchange membrane divides the electrolytic cell into anode chamber (containing counter electrodes) and cathode chamber (containing working and reference electrodes), whereas  $\text{CO}_2$  is reduced in the cathode chamber. Meanwhile, the entire reaction is in the airtight electrolytic cell, and the gas together with liquid-phase products can be collected separately for relevant detection and analysis after the reaction (Figure 7A).

Most basic research prefers to use H-type cells with a neutral liquid electrolyte. However, part of the H-type electrolytic cell, although possessing relatively good stability and ethylene yields, mostly requires a change of electrolyte and ion membrane after 12 to 20 h of operation, while maintaining the electrolyte in a vortex state during the  $\text{CO}_2\text{RR}$  reaction, which all limits its practical applicability (Table 1).

### Flow electrolytic cells

In contrast to H-type electrolytic cells, flow electrolytic cells do not require a reference electrode and usually consist of a gas cathode chamber, a cathode electrolyte chamber for the flow of the cathode electrolyte, and an anode chamber for the oxygen evolution reaction (OER), of which the gas diffusion electrode (GDE, containing a catalyst) separates the reaction gas from the cathode electrolyte chamber. This electrolytic cell effectively solves the problem of low  $\text{CO}_2$  solubility in aqueous solutions by separating the  $\text{CO}_2$  from the electrolyte. In addition, the reactants and products can be circulated in and out of the electrode, which greatly improves the efficiency of  $\text{CO}_2$  mass transfer. The development of this electrolytic cell thus offers the possibility of industrial applications of  $\text{CO}_2$  reduction reactions.

The flow electrolytic cell has a wider choice of electrolytes, but it can be concerned that the ethylene yield of the flow electrolytic cell is not ideal compared with that of the H-type electrolytic cell, as it is currently limited mainly by the preparation and performance retention of the GDE. Since the adhesion of the catalyst to the substrate and the GDE is hit by molecules from the gas and liquid in the reaction, which is not

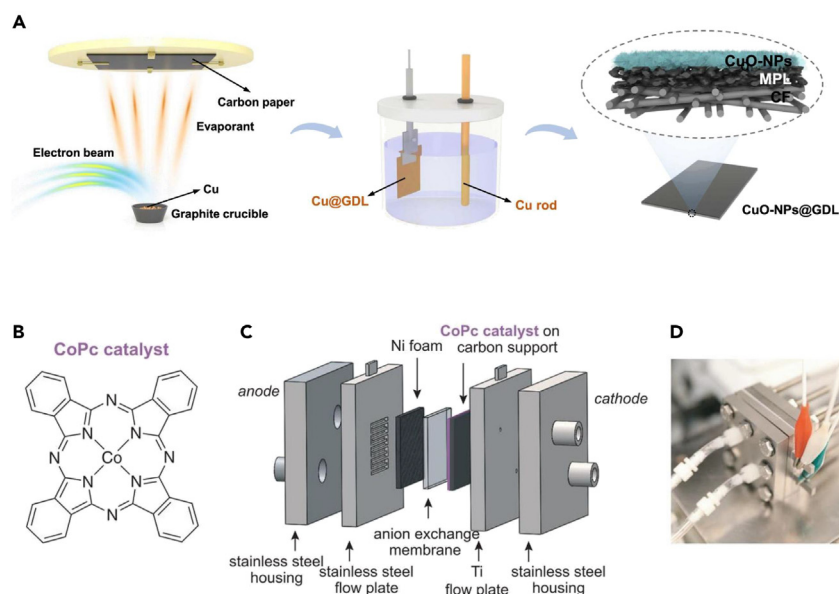


**Figure 7. Type of electrolytic cell**

(A) Schematic illustration of the electrolytic cells.<sup>34</sup> Copyright 2022, Nature Communications.

(B–D) Membrane flow reactor for efficient CO<sub>2</sub>RR with a cobalt-based molecular electrocatalyst.<sup>43</sup>

conductive to the GDE long-term retention performance and thus restricts the effective operation of the flow electrolytic cell, maintaining hydrophobic performance and retarding degradation of performance are outstanding issues for GDE (Table 2).

### Membrane electrode assembly cell

Compared with the flow electrolytic cell, the MEA cell is divided into a cathode chamber and an anode chamber by an ion exchange membrane. The cathode GDE and anode catalyst are located on opposite sides of the membrane (Figures 7B–7D). Moreover, the cathode side may not need liquid electrolyte, and the H<sub>2</sub>O required for the reaction may be supplied by the moist reaction gas or anode electrolyte.

MEA cells are not often used in basic research because of their high price and technical requirements, but they are still of great commercial value. Most existing studies have selected Ti-IrO<sub>2</sub> as the substrate; in addition, due to its adoption of a non-liquid electrolyte at the cathode, it greatly avoids the problems of carbon corrosion, hydrophobic loss, binder dissolution, and overflow in flowing electrolytic cells, but the provision of OH<sup>-</sup> and catalyst design are issues that need to be addressed for MEA cell (Table 3). Therefore, according to the design uses and application scenarios of the CO<sub>2</sub>RR electrolyte setup, the choice of catalyst, electrolytic cell, electrolyte, and input gas should also be determined on a case-by-case basis.

With the rapid development of CO<sub>2</sub>RR technology and the need for carbon neutrality, CO<sub>2</sub>RR is currently more focused on its commerciality, which can often be evaluated by current density, high conversion efficiency, and cost. Therefore, the selection, research, and development of electrolytic cells in the future should be more simulated in commercial environments. The entire CO<sub>2</sub>RR reaction environment of the H-type electrolytic cell is in a relatively closed state, with the working electrode immersed in the electrolyte, and the relatively stable initial environment of the reaction. At this time, the selectivity of catalyst catalyzed CO<sub>2</sub> into ethylene is stable. As the reaction progresses, the liquid product accumulates in the electrolyte, the catalyst gradually corrodes or fails, and the anode chamber HER product increases, thereby affecting the CO<sub>2</sub>RR progress, the selectivity of ethylene gradually decreases until the electrolytic cell fails. The current density that can pass through the whole process is much lower than that of flow cells and MEA cells, but the selectivity of ethylene is excellent in a short time. However, the entire CO<sub>2</sub>RR reaction environment of the flow electrolytic cell and MEA cell is in a relative cyclic state, but because the catalyst reacts with the reactant CO<sub>2</sub> in the relative flow state, the adsorption capacity of the intermediate is limited, so the selectivity of ethylene is relatively low. Among them, MEA cells containing solid electrolytes are a favorable direction for the future production of liquid products.

## DISCUSSION

In recent years, because of the greenhouse gas emissions, environmental changes, and the energy crisis and other real problems, the efficient use of resources and recyclable regeneration has become a hot research direction. From the use of straw, grass, agricultural waste, etc. after fermentation and other processing into biofuels or bio-based polymers,<sup>52</sup> to today's catalytic CO<sub>2</sub>, CO, H<sub>2</sub>, and other gas redox reactions to produce formic acid, ethylene, and other energy, the use of biological resources to produce carbon-based consumer products has gradually become a reality.<sup>53</sup> From the beginning, bioproduction of ethylene had no cost competitiveness compared with petrochemical-derived ethylene. Since 2008, the economic benefits of bio-polyethylene have continuously increased. Although, the current capacity of copper

**Table 1. Summary of the composition, stability, and catalytic capacity of representative H-type cells**

| Cathode catalyst <sup>ref</sup>  | Gas feed                              | Ion exchange membrane        | Electrolyte (pH)                     | FE <sub>ethylene</sub> (or C <sub>2</sub> H <sub>4</sub> production rate) and current density (cathode/cell potential) | Stability (h) |
|----------------------------------|---------------------------------------|------------------------------|--------------------------------------|--|---------------|
| A-CuNWs <sup>30</sup>            | CO <sub>2</sub>                       | Nafion ion exchange membrane | 0.1 M KHCO <sub>3</sub>              | 77.40% ± 3.16%<br>−0.97 to −1.07 V   | ~200          |
| DVL-Cu <sup>34</sup>             | CO <sub>2</sub>                       | Nafion 117 membrane          | 0.5 M KCl                            | 84.5% ± 1.7%<br>−0.9 V   | ~50           |
| OBC <sup>26</sup>                | CO <sub>2</sub>                       | Nafion 117 membrane          | 0.5 M KHCO <sub>3</sub> (7.2)        | 45%<br>−0.95 V   | –             |
| CuOx-NiNC (1:2) <sup>41</sup>    | CO <sub>2</sub> /CO                   | —                            | 0.1 M KHCO <sub>3</sub> (6.9)        | ~3.75 nmol cm <sup>−2</sup> s <sup>−1</sup><br>−0.84 V <sub>RHE</sub>  | —             |
| polycrystalline Cu <sup>45</sup> | CO <sub>2</sub> /O <sub>2</sub> (8:2) | Selemon AMV membrane         | 0.1 M KHCO <sub>3</sub>              | Over 170-fold increase in ethylene production rate<br>−0.75V <sub>RHE</sub>  | —             |
| n-CuNS <sup>31</sup>             | CO <sub>2</sub>                       | Nafion 117 membrane          | 0.1 M K <sub>2</sub> SO <sub>4</sub> | 80%<br>−1.18V (versus RHE)   | 14            |

nanocatalysts to produce C<sub>2+</sub> products in electrolytic cells is still not enough for the energy and chemical industries, but it may be able to apply it to food science, such as fruit and vegetable ripening regulation, food packaging materials, etc. Agricultural production and processing of agricultural products also emit a certain amount of CO<sub>2</sub>, CO, and other gases, and the use of these gases to improve ecological recycling efficiency is also a promising application.

As a plant hormone, ethylene acts as an important regulator in plant growth and development and physiological responses, whereas ethylene production is mainly affected by the transcription and translation of both ACS and ACO enzyme genes as well as ACC homeostasis. Ethylene production in plants increases significantly during the plant life cycle such as fertilization, maturation, senescence and in the response to biotic and abiotic stresses.<sup>54</sup> Normally, only trace amounts of ethylene are present in plants. However, there are two ethylene synthesis systems in higher plants, including an auto-inhibitory mechanism (system I) and an auto-catalytic mechanism (system II), and differences in the expression of ACS genes affect the shift in the ethylene synthesis system in fruits.<sup>55</sup> Because ethylene is closely related to fruit ripening, it is often used as a ripening agent for avocado, kiwi, and other fruits. At the same time, 1-methylcyclopropene (1-MCP), low temperature, 6-benzylaminopurine (6-BA),<sup>56</sup> and melatonin<sup>57</sup> are often used to inhibit ethylene production in fruits and vegetables during storage and transportation and extend the time to market by regulating the amount of ethylene released from fruits and vegetables in order to improve their commercial value. However, ethephon has pesticide abuse and poisoning problems, and ethylene is not easy to store, and electrochemical CO<sub>2</sub> reduction technology can regulate ethylene production on and off electricity, and participate in the ripening of fruits and vegetables in the form of exogenous ethylene to achieve green and safe in the whole process, so as to avoid the drawbacks of the above fruit and vegetable ripening control methods.

Furthermore, ethylene is currently an important raw material for the production of plastic products, while plastic packaging and plastic films are widely used as food packaging materials, including polyethylene (PE), polyvinyl chloride (PVC), and polystyrene (PS). However, due to the pollution of the ocean, soil, and organisms by plastics as well as the problem of petroleum resources, bio-based plastics have

**Table 2. Summary of the composition, stability, and catalytic capacity of representative flow-through electrolytic cells**

| Cathode catalyst <sup>ref</sup>                             | Gas feed        | GDL/substrate                                | Electrolyte (pH)                      | FE <sub>ethylene</sub> (or C <sub>2</sub> H <sub>4</sub> production rate) and current density (or cathode/cell potential) | Stability (h)                 |
|---|-----------------|--|---------------------------------------|---|-------------------------------|
| DVL-Cu <sup>34</sup>  | CO <sub>2</sub> | DVL-Cu/Carbon paper                          | Catholyte: KCl<br>Anolyte: KOH        | 84.5% ± 1.7%<br>−0.81 V   | ~55                           |
| 2-dimensional Cu(II) oxide nanosheet (CuO NS) <sup>27</sup> | CO <sub>2</sub> | 2D CuO NS/Freudenberg C2 gas diffusion layer | Catholyte:<br>0.1 M KHCO <sub>3</sub> | 65%<br>700 mA cm <sup>−2</sup>  | 24 (300 mA cm <sup>−2</sup> ) |
| Cu-P1 (P1 = poly-N-(6-aminohexyl)acrylamide) <sup>37</sup>  | CO <sub>2</sub> | Cu-P1/IrO <sub>2</sub>                       | 1 M KOH                               | 72%<br>−0.97V   | 3                             |
| CuCl <sub>2</sub> /cellulose/CP <sup>32</sup>               | CO <sub>2</sub> | CuCl <sub>2</sub> /cellulose/CP/PTFE         | 10 M KOH                              | ~45%<br>−0.517V <sub>RHE</sub>  | ~30                           |

**Table 3. Summary of the composition, stability, and catalytic capacity of representative MEA cells**

| Cathode Catalyst <sup>ref</sup> | Gas feed        | GDL/substrate   | Anolyte electrolyte (pH) | FE <sub>ethylene</sub> (or C <sub>2</sub> H <sub>4</sub> production rate) and current density (or cathode/cell potential) | Stability (h) |
|---------------------------------|-----------------|---|--------------------------|---|---------------|
| DVL-Cu <sup>34</sup>            | CO <sub>2</sub> | CuO-NPs@GDL/<br>Sustainion X37-50/Ti-IrO <sub>2</sub> | 0.5 M KHCO <sub>3</sub>  | 80.0% ± 2.2%<br>200 mA cm <sup>-2</sup>   | —             |
| Nano-Cu <sup>50</sup>           | CO <sub>2</sub> | Cu (5N high purity)/QAPEEK                            | Pure water               | 48%<br>308 mA cm <sup>-2</sup>  | 5             |

received widespread attention because of their bio-resource utilization and biodegradability. Currently, glucose from sugar cane, corn, and other biological raw materials is often used for fermentation to produce ethylene monomer and then polymerized into the corresponding plastic.<sup>58</sup> Meanwhile, natural ethylene inhibitors, active materials, controlled ripening technologies, and biodegradable bio-based plastics related to ethylene still have great potential for development in the food science field because of people's habits and need of change, as well as the concern for environmental protection and renewable resources.

In addition to electrocatalytic CO<sub>2</sub> reduction to ethylene, photocatalytic and biocatalytic<sup>59</sup> CO<sub>2</sub> reduction to high-value-added products can also be tried for application in food science. Currently, photocatalysis is mostly used for ethylene removal in food preservation, with researchers using TiO<sub>2</sub> or Pt as the main raw material to make nanofilms that oxidize ethylene under UV light or sunlight to generate CO<sub>2</sub> for removal. Meanwhile, high-performance metal ethylene detectors based on palladium loaded have also been studied.<sup>60</sup> If such ideas are arranged, it may be possible to simplify the current ripening control techniques, devices, and applicable environments.

### Limitations of the study

In the low-carbon era, CO<sub>2</sub>RR and CORR are uniquely positioned to "carbon neutralization". Currently, electrocatalytic CO<sub>2</sub> reduction reactions are limited by the stability of the catalyst and electrolytic cell reactor performance, cost, and the reaction environment, which makes them difficult to apply in practical production, but by trying to translate existing excellent catalytic technologies into products in areas where higher efficiency and stability are not required, better optimizations may be found in practical applications.

### ACKNOWLEDGMENTS

This work was supported by the National Key Research and Development Program of China (No. 2022YFF1100900), the Natural Science Foundation of China (No. 22077126), and the Beijing Nova Program (No. 20220484021).

### AUTHOR CONTRIBUTIONS

Conceptualization, Y.X.D. and L.B.L.; formal analysis, Y.X.D., B.F., Y.X.L., and X.F.W.; investigation, Y.X.D. and M.M.; writing—original draft, Y.X.D. and Y.X.D.; writing—review & editing, Y.X.D., Y.X.D., M.M., and L.L.L.; Supervision, L.B.L. and F.Z.R.

### DECLARATION OF INTERESTS

The authors declare that they have no known competing financial interests or personal relationships that could have appeared to influence the work reported in this paper.

### REFERENCES

- Friedlingstein, P., O'Sullivan, M., Jones, M.W., Andrew, R.M., Hauck, J., Olsen, A., Peters, G.P., Peters, W., Pongratz, J., Sitch, S., et al. (2020). Global Carbon Budget 2020. *Earth Syst. Sci. Data* 12, 3269–3340.
- Cai, Y., Sam, C.Y., and Chang, T. (2018). Nexus between clean energy consumption, economic growth and CO<sub>2</sub> emissions. *J. Clean. Prod.* 182, 1001–1011.
- Yang, W., Min, Z., Yang, M., and Yan, J. (2022). Exploration of the implementation of carbon neutralization in the field of natural resources under the background of sustainable Development—An overview. *Int. J. Env. Res. Pub. He.* 19, 14109.
- Coskun, H., Aljabour, A., De Luna, P., Farka, D., Greunz, T., Stifter, D., Kus, M., Zheng, X., Liu, M., Hassel, A.W., et al. (2017). Biofunctionalized conductive polymers enable efficient CO<sub>2</sub> electroreduction. *Sci. Adv.* 3, e1700686.
- Lin, L., Wang, K., Yang, K., Chen, X., Fu, X., and Dai, W. (2017). The visible-light-assisted thermocatalytic methanation of CO<sub>2</sub> over Ru/TiO(2-X)NX. *Appl. Catal. B Environ.* 204, 440–455.
- Esmailirad, M., Baskin, A., Kondori, A., Sanz-Matias, A., Qian, J., Song, B., Tamadoni Saray, M., Kucuk, K., Belmonte, A.R., Delgado, P.N.M., et al. (2021). Gold-like activity copper-like selectivity of heteroatomic transition metal carbides for electrocatalytic carbon dioxide reduction reaction. *Nat. Commun.* 12, 5067.
- Yang, D., Yu, H., He, T., Zuo, S., Liu, X., Yang, H., Ni, B., Li, H., Gu, L., Wang, D., and Wang, X. (2019). Visible-light-switched electron transfer over single porphyrin-metal atom center for highly selective electroreduction of carbon dioxide. *Nat. Commun.* 10, 3844.
- Pan, Y., Zhang, H., Zhang, B., Gong, F., Feng, J., Huang, H., Vanka, S., Fan, R., Cao, Q., Shen, M., et al. (2023). Renewable formate from sunlight, biomass and carbon dioxide in a photoelectrochemical cell. *Nat. Commun.* 14, 1013.
- Huang, Q., Niu, Q., Li, X.F., Liu, J., Sun, S.N., Dong, L.Z., Li, S.L., Cai, Y.P., and Lan, Y.Q. (2022). Demystifying the roles of single metal site and cluster in CO<sub>2</sub> reduction via light and electric dual-responsive polyoxometalate-based metal-organic frameworks. *Sci. Adv.* 8, eadd5598.
- Merchante, C., Vallarino, J.G., Osorio, S., Aragüez, I., Villarreal, N., Ariza, M.T., Martínez, G.A., Medina-Escobar, N., Civallo, M.P., Fernie, A.R., et al. (2013). Ethylene is involved in strawberry fruit ripening in an

- organ-specific manner. *J. Exp. Bot.* **64**, 4421–4439.
- Russo, E., and Villa, C. (2019). Poloxamer hydrogels for biomedical applications. *Pharmaceutics* **11**, 671.
  - Gautam, H., Fatma, M., Sehar, Z., Iqbal, N., Albaqami, M., and Khan, N.A. (2022). Exogenously-sourced ethylene positively modulates photosynthesis, carbohydrate metabolism, and antioxidant defense to enhance heat tolerance in rice. *Int. J. Mol. Sci.* **23**, 1031.
  - Zhang, W., and Wen, C.K. (2010). Preparation of ethylene gas and comparison of ethylene responses induced by ethylene, ACC, and ethephon. *Plant Physio. Bioch.* **48**, 45–53.
  - Zhong, H., Ghorbani-Asl, M., Ly, K.H., Zhang, J., Ge, J., Wang, M., Liao, Z., Makarov, D., Zscheck, E., Brunner, E., et al. (2020). Synergistic electroreduction of carbon dioxide to carbon monoxide on bimetallic layered conjugated metal-organic frameworks. *Nat. Commun.* **11**, 1409.
  - Liang, Z., Song, L., Sun, M., Huang, B., and Du, Y. (2021). Tunable CO/H<sub>2</sub> ratios of electrochemical reduction of CO<sub>2</sub> through the zn-In dual atomic catalysts. *Sci. Adv.* **7**, eabl4915.
  - Gao, Y., Yang, R., Wang, C., Liu, C., Wu, Y., Li, H., and Zhang, B. (2022). Field-induced reagent concentration and sulfur adsorption enable efficient electrocatalytic semihydrogenation of alkynes. *Sci. Adv.* **8**, eabm9477.
  - Ko, Y.J., Kim, J.Y., Lee, W.H., Kim, M.G., Seong, T.Y., Park, J., Jeong, Y., Min, B.K., Lee, W.S., Lee, D.K., and Oh, H.S. (2022). Exploring dopant effects in stannic oxide nanoparticles for CO<sub>2</sub> electro-reduction to formate. *Nat. Commun.* **13**, 2205.
  - Yang, F., Elnabawy, A.O., Schimmenti, R., Song, P., Wang, J., Peng, Z., Yao, S., Deng, R., Song, S., Lin, Y., et al. (2020). Bismuthene for highly efficient carbon dioxide electroreduction reaction. *Nat. Commun.* **11**, 1088.
  - Hung, S.F., Xu, A., Wang, X., Li, F., Hsu, S.H., Li, Y., Wicks, J., Cervantes, E.G., Rasouli, A.S., Li, Y.C., et al. (2022). A metal-supported single-atom catalytic site enables carbon dioxide hydrogenation. *Nat. Commun.* **13**, 819.
  - Dong, C., Lian, C., Hu, S., Deng, Z., Gong, J., Li, M., Liu, H., Xing, M., and Zhang, J. (2018). Size-dependent activity and selectivity of carbon dioxide photocatalytic reduction over platinum nanoparticles. *Nat. Commun.* **9**, 1252.
  - Niu, K., Xu, Y., Wang, H., Ye, R., Xin, H.L., Lin, F., Tian, C., Lum, Y., Bustillo, K.C., Doeff, M.M., et al. (2017). A spongy nickel-organic CO<sub>2</sub> reduction photocatalyst for nearly 100% selective CO production. *Sci. Adv.* **3**, e1700921.
  - Qin, T., Qian, Y., Zhang, F., and Lin, B.L. (2019). Chloride-derived copper electrode for efficient electrochemical reduction of CO<sub>2</sub> to ethylene. *Chin. Chem. Lett.* **30**, 314–318.
  - Schlögl, R. (2015). Heterogeneous catalysis. *Angew. Chem. Int. Ed. Engl.* **54**, 3465–3520.
  - Shao, W., Li, X., Zhu, J., Zu, X., Liang, L., Hu, J., Pan, Y., Zhu, J., Yan, W., Sun, Y., and Xie, Y. (2022). Metal<sup>n+</sup>-Metal<sup>l+</sup> pair sites steer C-C coupling for selective CO<sub>2</sub> photoreduction to C<sub>2</sub> hydrocarbons. *Nano Res.* **15**, 1882–1891.
  - Yuan, X., Chen, S., Cheng, D., Li, L., Zhu, W., Zhong, D., Zhao, Z.J., Li, J., Wang, T., and Gong, J. (2021). Controllable Cu<sup>0</sup>-Cu<sup>+</sup> sites for electrocatalytic reduction of carbon dioxide. *Angew. Chem. Int. Ed. Engl.* **60**, 15344–15347.
  - Zhang, W., Huang, C., Xiao, Q., Yu, L., Shuai, L., An, P., Zhang, J., Qiu, M., Ren, Z., and Yu, Y. (2020). Atypical oxygen-bearing copper boosts ethylene selectivity toward electrocatalytic CO<sub>2</sub> reduction. *J. Am. Chem. Soc.* **142**, 11417–11427.
  - Wang, X., Klingan, K., Klingenhof, M., Möller, T., Ferreira de Araújo, J., Martens, I., Bagger, A., Jiang, S., Rossmeisl, J., Dau, H., and Strasser, P. (2021). Morphology and mechanism of highly selective Cu(II) oxide nanosheet catalysts for carbon dioxide electroreduction. *Nat. Commun.* **12**, 794.
  - Yang, B., Liu, K., Li, H., Liu, C., Fu, J., Li, H., Huang, J.E., Ou, P., Alkayali, T., Cai, C., et al. (2022). Accelerating CO electroreduction to multicarbon products via synergistic Electric-Thermal field on copper nanoneedles. *J. Am. Chem. Soc.* **144**, 3039–3049.
  - Wakerley, D., Lamaison, S., Ozanam, F., Menguy, N., Mercier, D., Marcus, P., Fontecave, M., and Mougél, V. (2019). Bio-inspired hydrophobicity promotes CO<sub>2</sub> reduction on a Cu surface. *Nat. Mater.* **18**, 1222–1227.
  - Choi, C., Kwon, S., Cheng, T., Xu, M., Tieu, P., Lee, C., Cai, J., Lee, H.M., Pan, X., Duan, X., et al. (2020). Highly active and stable stepped Cu surface for enhanced electrochemical CO<sub>2</sub> reduction to C<sub>2</sub>H<sub>4</sub>. *Nat. Catal.* **3**, 804–812.
  - Zhang, B., Zhang, J., Hua, M., Wan, Q., Su, Z., Tan, X., Liu, L., Zhang, F., Chen, G., Tan, D., et al. (2020). Highly electrocatalytic ethylene production from CO<sub>2</sub> on nanodeficient Cu nanosheets. *J. Am. Chem. Soc.* **142**, 13606–13613.
  - Song, J.Y., Kim, C., Kim, M., Cho, K.M., Gereige, I., Jung, W.B., Jeong, H., and Jung, H.T. (2021). Generation of high-density nanoparticles in the carbothermal shock method. *Sci. Adv.* **7**, eabk2984.
  - Jiang, Y., Wang, X., Duan, D., He, C., Ma, J., Zhang, W., Liu, H., Long, R., Li, Z., Kong, T., et al. (2022). Structural reconstruction of Cu<sub>2</sub>O superparticles toward electrocatalytic CO<sub>2</sub> reduction with high C<sub>2+</sub> products selectivity. *Adv. Sci.* **9**, 2105292.
  - Liu, W., Zhai, P., Li, A., Wei, B., Si, K., Wei, Y., Wang, X., Zhu, G., Chen, Q., Gu, X., et al. (2022). Electrochemical CO<sub>2</sub> reduction to ethylene by ultrathin CuO nanoplate arrays. *Nat. Commun.* **13**, 1877.
  - Mu, S., Lu, H., Wu, Q., Li, L., Zhao, R., Long, C., and Cui, C. (2022). Hydroxyl radicals dominate reoxidation of oxide-derived Cu in electrochemical CO<sub>2</sub> reduction. *Nat. Commun.* **13**, 3694.
  - Li, F., Thevenon, A., Rosas-Hernández, A., Wang, Z., Li, Y., Gabardo, C.M., Ozden, A., Dinh, C.T., Li, J., Wang, Y., et al. (2020). Molecular tuning of CO<sub>2</sub>-to-ethylene conversion. *Nature* **577**, 509–513.
  - Chen, X., Chen, J., Alghorabi, N.M., Henckel, D.A., Zhang, R., Nwabara, U.O., Madsen, K.E., Kenis, P.J.A., Zimmerman, S.C., and Gewirth, A.A. (2020). Electrochemical CO<sub>2</sub>-to-ethylene conversion on polyamine-incorporated Cu electrodes. *Nat. Catal.* **4**, 20–27.
  - Lim, C.Y.J., Yilmaz, M., Arce-Ramos, J.M., Handoko, A.D., Teh, W.J., Zheng, Y., Khoo, Z.H.J., Lin, M., Isaacs, M., Tam, T.L.D., et al. (2023). Surface charge as activity descriptors for electrochemical CO<sub>2</sub> reduction to multi-carbon products on organic-functionalised Cu. *Nat. Commun.* **14**, 335.
  - Malkani, A.S., Li, J., Oliveira, N.J., He, M., Chang, X., Xu, B., and Lu, Q. (2020). Understanding the electric and nonelectric field components of the cation effect on the electrochemical CO reduction reaction. *Sci. Adv.* **6**, eabd2569.
  - Wang, Q., Liu, K., Hu, K., Cai, C., Li, H., Li, H., Herran, M., Lu, Y.R., Chan, T.S., Ma, C., et al. (2022). Attenuating metal-substrate conjugation in atomically dispersed nickel catalysts for electroreduction of CO<sub>2</sub> to CO. *Nat. Commun.* **13**, 6082.
  - Wang, X., de Araújo, J.F., Ju, W., Bagger, A., Schmies, H., Kühl, S., Rossmeisl, J., and Strasser, P. (2019). Mechanistic reaction pathways of enhanced ethylene yields during electroreduction of CO<sub>2</sub>-CO co-feeds on Cu and Cu-tandem electrocatalysts. *Nat. Nanotechnol.* **14**, 1063–1070.
  - Wang, Q., Dai, M., Li, H., Lu, Y.R., Chan, T.S., Ma, C., Liu, K., Fu, J., Liao, W., Chen, S., et al. (2023). Asymmetric coordination induces electron localization at ca sites for robust CO<sub>2</sub> electroreduction to CO. *Adv. Mater.* **35**, e2300695.
  - Ren, S., Joulé, D., Salvatore, D., Torbensen, K., Wang, M., Robert, M., and Berlinguette, C.P. (2019). Molecular electrocatalysts can mediate fast, selective CO<sub>2</sub> reduction in a flow cell. *Science* **365**, 367–369.
  - Choi, C., Wang, X., Kwon, S., Hart, J.L., Rooney, C.L., Harmon, N.J., Sam, Q.P., Cha, J.J., Goddard, W.A., 3rd, Elimelech, M., and Wang, H. (2023). Efficient electrocatalytic valorization of chlorinated organic water pollutant to ethylene. *Nat. Nanotechnol.* **18**, 160–167.
  - He, M., Li, C., Zhang, H., Chang, X., Chen, J.G., Goddard, W.A., 3rd, Cheng, M.J., Xu, B., and Lu, Q. (2020). Oxygen induced promotion of electrochemical reduction of CO<sub>2</sub> via co-electrolysis. *Nat. Commun.* **11**, 3844.
  - Wang, Y., Wang, Z., Dinh, C.T., Li, J., Ozden, A., Golam Kibria, M., Seifitokaldani, A., Tan, C.S., Gabardo, C.M., Luo, M., et al. (2019). Catalyst synthesis under CO<sub>2</sub> electroreduction favours faceting and promotes renewable fuels electrosynthesis. *Nat. Catal.* **3**, 98–106.
  - Resasco, J., Chen, L.D., Clark, E., Tsai, C., Hahn, C., Jaramillo, T.F., Chan, K., and Bell, A.T. (2017). Promoter effects of alkali metal cations on the electrochemical reduction of carbon dioxide. *J. Am. Chem. Soc.* **139**, 11277–11287.
  - Lv, J.J., Jouny, M., Luc, W., Zhu, W., Zhu, J.J., and Jiao, F. (2018). A highly porous copper electrocatalyst for carbon dioxide reduction. *Adv. Mater.* **30**, e1803111.
  - Li, J., Guo, J., and Dai, H. (2022). Probing dissolved CO<sub>2</sub>(aq) in aqueous solutions for CO<sub>2</sub> electroreduction and storage. *Sci. Adv.* **8**, eabo0399.
  - Li, W., Yin, Z., Gao, Z., Wang, G., Li, Z., Wei, F., Wei, X., Peng, H., Hu, X., Xiao, L., et al. (2022). Bifunctional ionomers for efficient co-electrolysis of CO<sub>2</sub> and pure water towards ethylene production at industrial-scale current densities. *Nat. Energy* **7**, 835–843.
  - Sanchez-Diez, E., Ventosa, E., Guarnieri, M., Trovo, A., Flox, C., Marcilla, R., Soavi, F., Mazur, P., Aranzabe, E., and Ferret, R. (2020).

- Redox flow batteries: Status and perspective towards sustainable stationary energy storage. *J. Power Sources* 481, 228804.
52. Cywar, R.M., Rorrer, N.A., Hoyt, C.B., Beckham, G.T., and Chen, E.Y.X. (2021). Bio-based polymers with performance-advantaged properties. *Nat. Rev. Mater.* 7, 83–103.
  53. Tuck, C.O., Pérez, E., Horváth, I.T., Sheldon, R.A., and Poliakoff, M. (2012). Valorization of biomass: Deriving more value from waste. *Science* 337, 695–699.
  54. Li, S., Chen, K., and Grierson, D. (2019). A critical evaluation of the role of ethylene and MADS transcription factors in the network controlling fleshy fruit ripening. *New Phytol.* 221, 1724–1741.
  55. Barry, C.S., Llop-Tous, M.I., and Grierson, D. (2000). The regulation of 1-aminocyclopropane-1-carboxylic acid synthase gene expression during the transition from system-1 to system-2 ethylene synthesis in tomato. *Plant Physiol.* 123, 979–986.
  56. Zhang, Y., Gao, Z., Hu, M., Pan, Y., Xu, X., and Zhang, Z. (2022). Delay of ripening and senescence in mango fruit by 6-benzylaminopurine is associated with inhibition of ethylene biosynthesis and membrane lipid catabolism. *Postharvest Biol. Tec.* 185, 111797.
  57. Liu, S., Huang, H., Huber, D.J., Pan, Y., Shi, X., and Zhang, Z. (2020). Delay of ripening and softening in ‘Guifei’ mango fruit by postharvest application of melatonin. *Postharvest Biol. Tec.* 163, 111136.
  58. Tokala, V.Y., Singh, Z., and Kyaw, P.N. (2021). Postharvest fruit quality of apple influenced by ethylene antagonist fumigation and ozonized cold storage. *Food Chem.* 341, 128293.
  59. Yu, W., Zeng, Y., Wang, Z., Xia, S., Yang, Z., Chen, W., Huang, Y., Lv, F., Bai, H., and Wang, S. (2023). Solar-powered multi-organism symbiont mimic system for beyond natural synthesis of polypeptides from CO<sub>2</sub> and N<sub>2</sub>. *Sci. Adv.* 9, eadf6772.
  60. Zhao, Q., Duan, Z., Yuan, Z., Li, X., Si, W., Liu, B., Zhang, Y., Jiang, Y., and Tai, H. (2020). High performance ethylene sensor based on palladium-loaded tin oxide: Application in fruit quality detection. *Chin. Chem. Lett.* 31, 2045–2049.